

- quium on Venus, LPI Contrib. No. 789, pp. 116-117.
- Solomon, S. C., et al. 1992. Venus tectonics: An overview of Magellan observations. *J. Geophys. Res.* 97:13199-13256.
- Squires, S. W., et al. 1992a. The morphology and evolution of coronae on Venus. *J. Geophys. Res.* 97:13611-13634.
- Squires, S. W., et al. 1992b. The spatial distribution of coronae on Venus. In *International Colloquium on Venus*, LPI Contrib. No. 789, pp. 119-120.
- Stefanick, M., and Jurdy, D. M. 1984. The distribution of hot spots. *J. Geophys. Res.* 89:9919-9925.
- Stofan, E. R., and Head, J. W. 1990. Coronae of Mnemosyne Regio: Morphology and origin. *Icarus* 83:216-243.
- Stofan, E. R., and Saunders, R. S. 1990. Geologic evidence of hotspot activity on Venus: Predictions for Magellan. *Geophys. Res. Lett.* 17:1377-1380.
- Stofan, E. R., Bindshadler, D. L., Head, J. W., and Parmentier, E. M. 1991. Coronae structure on Venus: Models of origin. *J. Geophys. Res.* 96:20933-20946.
- Stofan, E. R., et al. 1992. Global distribution and characteristics of coronae and related features on Venus: Implications for origin and relation to mantle processes. *J. Geophys. Res.* 97:13347-13378.
- Stofan, E. R., Smrekar, S. E., Bindshadler, D. L., and Senske, D. A. 1996. Large topographic rises on Venus: Implications for mantle upwelling. *J. Geophys. Res.*, in press.
- Strom, R. G., Schaber, G. G., and Dawson, D. 1994. The global resurfacing of Venus. *J. Geophys. Res.* 99:10899-10926.
- Takada, A. 1989. Magma transport and reservoir formation by a system of propagating cracks. *Bull. Volc.* 52:118-126.
- Thornhill, G. D. 1993. Theoretical modeling of eruption plumes on Venus. *J. Geophys. Res.* 98:9107-9111.
- Tsukui, M., Sakuyama, M., Koyaguchi, T., and Ozawa, K. 1986. Long-term eruption rates and dimensions of magma reservoirs beneath quaternary polygenetic volcanoes in Japan. *J. Volc. Geotherm. Res.* 29:189-202.
- Turcotte, D. L. 1993. An episodic hypothesis for Venusian tectonics. *J. Geophys. Res.* 98:17061-17068.
- Walker, G. P. L. 1984. Downsize calderas, ring faults, caldera sizes, and incremental caldera growth. *J. Geophys. Res.* 84:8407-8415.
- Ward, W. R., Burns, J. A., and Toon, O. B. 1979. Past obliquity oscillations of Mars: The role of the Tharsis uplift. *J. Geophys. Res.* 84:243-259.
- White, R. S. 1992. Magmatism during and after continental break-up. In *Magmatism and the Causes of Continental Break-up*, eds. B. C. Storey, T. Alabaster and R. J. Pankhurst. GSA SP-68 (Boulder: Geological Soc. of America), p. 404.
- White, R. S., and McKenzie, D. 1989. Magmatism at rift zones: The generation of volcanic continental margins and flood basalts. *J. Geophys. Res.* 94:7685-7729.
- Wiles, C. R., and Foreshaw, M. R. B. 1992. Automated detection and measurements of small volcanoes on Venus. *Lunar Planet. Sci. Conf. XXIII:1527-1528* (abstract).
- Williams, H., and McBirney, A. R. 1979. *Volcanology* (San Francisco: Freeman Cooper).
- Wilson, L., and Head, J. W. 1994. Mars: Review and analysis of volcanic eruption theory and relationships to observed landforms. *Rev. Geophys.* 32(3):221-264.
- Wood, C. A. 1979. *Venusian Volcanism: Environmental Effects on Style and Landforms*. NASA TM-80339, pp. 244-246.
- Wood, C. A. 1984. Calderas: A planetary perspective. *J. Geophys. Res.* 89:8391-8406.

In Venus II Baughn et al. 1997,  
Univ. of Az Press, Tucson.

## CHANNELS AND VALLEYS

VICTOR R. BAKER and GORO KOMATSU  
*University of Arizona*

VIRGINIA C. GULICK  
*NASA Ames Research Center*

and

TIMOTHY J. PARKER  
*Jet Propulsion Laboratory*

More than 200 channels and valleys have been identified on the Magellan images of Venus. These are classified, on the basis of morphology, as simple channels (including sinuous rilles, simple channels with flow margins, and canali), complex channels (with or without flow margins), compound channels, and valley networks (including rectangular, labyrinthic, and pitted or irregular networks). Sinuous rilles closely resemble their lunar counterparts. Canali are exceptional for their remarkably constant width along very attenuated flow paths, exceeding 500 km. One of the compound channels, the outflow complex of Kallistos Vallis, extends over 1200 km and is up to 30 km wide. Venusian channels are globally distributed, but each class has a preferential topographic association. The canali are developed on the volcanic plains, while sinuous rilles occur at higher elevations, associated with volcanic complexes and coronae. Both canali and sinuous rilles have been deformed by post-emplacement tectonism. Highly fluid lavas, erupted at sustained, high discharges, seem best to explain many of the channel features, particularly for the canali and the compound channels. Explanation of the canali morphologies may also involve unusual low-viscosity lavas, perhaps of exotic composition.

## I. INTRODUCTION

Because liquid water was known to be unstable on the surface of Venus at current ambient conditions, the number and diversity of channels revealed on the surface of Venus by Magellan radar mapping was unexpected. The very first channel identified in Magellan imagery, later recognized as a canali-type channel, was sinuous, with constant width, no tributaries, no clear association with flow units, and extraordinary length (>500 km) (Head et al. 1991). This unique combination of characteristics has not been observed in terrestrial and Martian fluvial channels, nor in lava channels on the terrestrial planets. This anomaly attracted the attention of researchers who hypothesized diverse

mechanisms for the channel formation on Venus (Baker et al. 1992; Komatsu et al. 1992b; Gregg and Greeley 1993; Komatsu et al. 1993; Kargel et al. 1994; Bussey et al. 1995). As the mission progressed, researchers discovered a wide range of channel morphologies, including those more typical for lava channels on other terrestrial planets (Komatsu et al. 1993).

There are a number of Venusian channels similar in morphology to typical lava channels on the terrestrial planets. They have clear associations with flow units (levees/lateral flow deposits, or explained as flow margins in the classification of Komatsu et al. [1993]), and they tend to narrow and shallow downstream. Although these Venusian lava channels are commonly as much as an order of magnitude or two larger in scale than their counterparts on Earth, their mechanisms of formation can be considered analogous to those of terrestrial lava channels. Similar reasoning has been applied to the very large lava channels of Mars (Mouginis-Mark et al. 1992). The following discussion, therefore, focuses on the more unusual channels and valleys of Venus, such as canali, sinuous rilles, compound channels, and valley networks.

## II. CLASSIFICATION AND MORPHOLOGY

### A. Channels

More than 200 channels and valleys have been identified on the Magellan images of Venus. Of these there are approximately a dozen valley networks and more than 200 channels exhibiting a wide variety of morphological characteristics. Preliminary classifications were presented by Gulick et al. (1991, 1992a), and Baker et al. (1992). These were subsequently updated by Komatsu et al. (1993). The morphological characteristics of the classification scheme are illustrated in Fig. 1. Channels will be discussed first, according to three types: (1) simple, (2) complex, and (3) compound.

*Simple Channels.* These are generally composed of a single main conduit which lacks complex branching and anastomosing (see Fig. 2 in Baker et al. 1992). Simple channels are further subdivided into sinuous rilles, simple channels with flow margins, and canali. Sinuous rilles are similar in morphology and size to those observed on the Moon (see Fig. 3a,b in Baker et al. 1992). They emanate from distinct, circular or elongated regions of collapse (generally several km in diameter); they are approximately 1 to 2 km wide and several tens of km long; and they become narrower and shallower distally. As on the Moon, most sinuous rilles on Venus are not associated with detectable lava flow margins. The morphological similarity between Venusian and lunar sinuous rilles suggests an origin by the thermal erosion of flowing lava (Hulme 1973, 1982). However, the exact origin of these channels could have been vastly different given that Venusian sinuous rilles tend to cluster on or near geologic features that are not found on the Moon, such as coronae, corona-like features, and arachnoids.

Some simple channels are located on well-defined flow deposits or flow fields (see Fig. 5 in Komatsu et al. 1993). These channels are somewhat

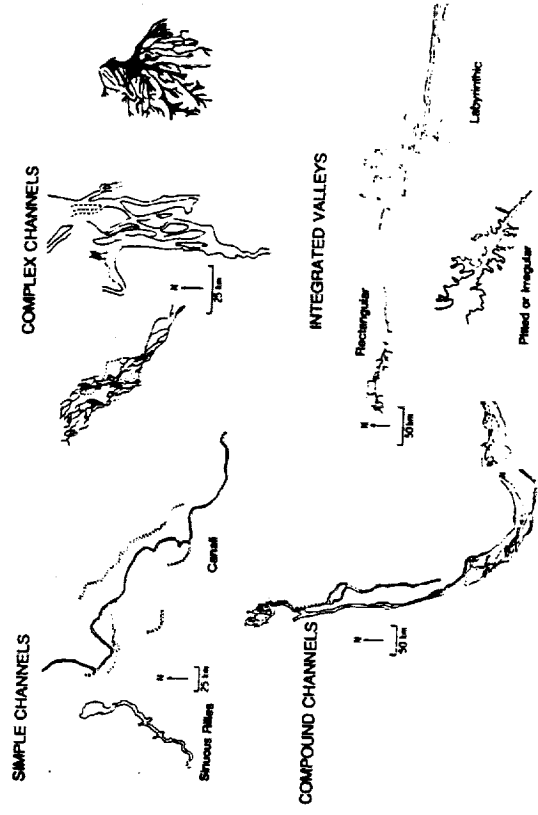


Figure 1. Morphological classification scheme of channels and valleys on Venus (figure updated from Gulick et al. 1992b).

similar to channels formed on terrestrial lava flows except that levees are usually not apparent on the Magellan radar imagery. Because these channels have formed entirely on lava flows and do not deeply incise surrounding terrain, they appear to be constructional in origin, similar to their terrestrial counterparts. In general, these simple channels exhibit indistinct source and terminal regions, in contrast to the Venusian sinuous rilles. Simple channels with flow margins commonly feed extensive lava flows associated with coronae, shield volcanoes, rift and fracture zones (Komatsu et al. 1993).

Canali are channels having a constant width and depth (Fig. 2). They are typically as wide as 3 km and are up to 500 km in length, although a few canali are as wide as 10 km, and the length reaches 6800 km in one case (see Fig. 6a in Komatsu et al. 1993). Canali may locally exhibit abandoned channel segments, cut-off meander bends, levees (see Fig. 5b in Baker et al. 1992) and radar dark terminal deposits (Gulick et al. 1991, 1992a). Sources and termini are generally indistinct. Canali are generally located in plains regions, particularly in Guinevere Planitia, Helen Planitia, as well as in the plains southeast of Artemis Planitia and north of Rusalka Planitia (Komatsu et al. 1993). Canali morphology suggests their probable formation by, and conveyance of, large discharges of low viscosity lava to distant regions over prolonged periods (Komatsu et al. 1993).

*Complex Channels.* These form anastomosing, braided or distributary patterns that are usually, although not everywhere, on flow deposits (see Fig. 9 in Komatsu et al. 1993). Individual channel widths range from approximately

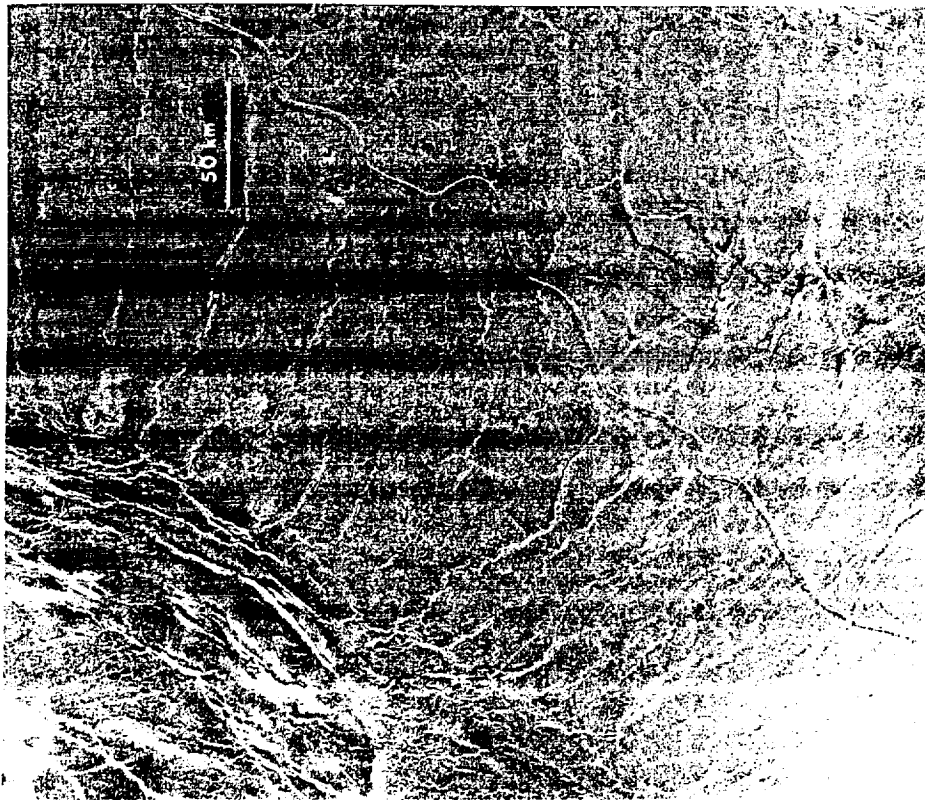


Figure 2. Radar image of Baltis Vallis, a canali-type channel located at 49° to 51° N, 165° to 168° E (S0N163; left-looking radar illumination). Channel width is approximately 1 to 4 km; scale bar equals 50 km. Baltis Vallis is the longest channel yet discovered in the solar system with a total length of ~6800 km.

3 km down to the limit of resolution, whereas the channel system may be 20 to 30 km wide and up to hundreds of km in length. Complex channels without associated flow deposits are commonly observed as segments of other channel types, such as the middle reach of a compound channel or as a subsidiary anastomosing, branching segment in a canali-type channel. The lack of related flow deposits suggests that these channels may be eroded into surrounding terrain. This particular subclass of complex channels is known simply as "complex channels without flow margins" (Komatsu et al., 1993).

also called "complex erosional channels" in Gulick et al., 1992a).

Most complex channels are located on flow deposits and are classified as complex channels with flow margins (Komatsu et al., 1993) (also called "complex constructional channels" in Gulick et al., 1992a). Channels are commonly separated by "islands" of radar-bright (or radar-dark in some cases) material (see Fig. 10b in Komatsu et al., 1993). Channel margins are sometimes lined with radar-bright material. Complex channels with flow margins are common on fluidized ejecta blankets (see Fig. 7a in Baker et al., 1992).

Complex channels are also located along with simple channels on lava flow deposits. For example, both complex and simple channels occur on the enormous flow deposits of Mylitta Fluctus (Roberts, 1992) in Lavinia Planitia (54° S, 353.4° E). Complex channels form delta-like distributary patterns along terminal reaches of flow deposits in Aphroditic Terra (see Fig. 7c,d in Baker et al., 1992).

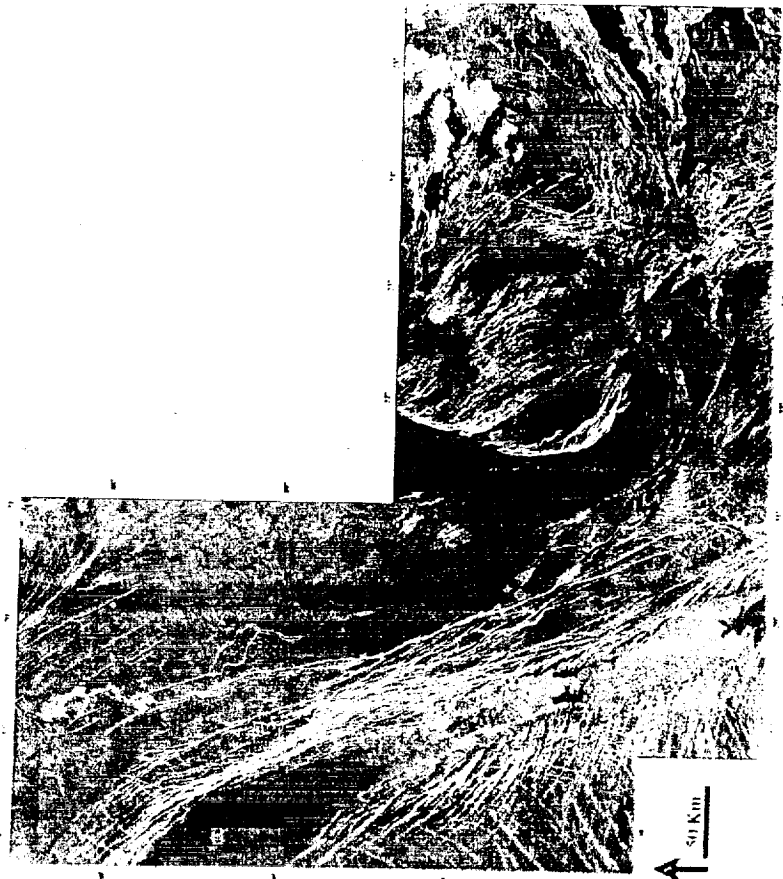


Figure 3. Portion of FMI DR 505021 (left-looking, Cycle 1) data coverage of Kadistis Vallis, from source collapse terrain (at top) through upper "distributary reach" (at right).

**Compound Channels.** These display both simple and complex segments (see Fig. 8 in Baker et al. 1992). Channels vary greatly in size, with widths ranging between several tens of km in complex regions down to the limit of resolution in simple reaches. Lengths of compound channels can range from 75 km to thousands of km. The upper segment of a compound channel commonly, although not in every case, resembles the morphology of a sinuous rille in that a single conduit emanates from a distinct collapsed region (Fig. 3). Instead of becoming narrower and shallowing distally, however, a compound channel bifurcates and anastomoses, resulting in stream-lined islands (Fig. 3). The lower reach may terminate in a flow deposit which can be quite extensive in some cases (Fig. 3). A detailed description of a representative compound channel, Kallistos Vallis, is provided in Sec. III.

### B. Valley Networks

The valley networks are distinct from the Venusian channels in that they lack bedforms that are direct indicators of fluid flow. These integrated valley systems are somewhat similar in morphology to those produced by groundwater sapping processes on Earth and Mars. Like their terrestrial and Martian counterparts, Venusian valley networks probably did not form by fluids being conveyed through conduits at bank-full stage. Instead, these landforms appear to have formed by the undermining and subsequent collapse of surface material by outflow of low-viscosity subsurface fluids, augmented by surface flow. The Venusian valley networks are divided into three morphological classes: (1) rectangular, (2) labyrinthic, and (3) pitted or irregular (Cullick et al. 1992a). Some networks display a morphology that is transitional between rectangular and labyrinthic. See Table I.

TABLE I  
Classification and Location of Valley Networks on Venus

Location	Type	Magellan Image	CTD-ROM
1. 3° N, 70.5° E	Rectangular	F-00N070	MG0009
2. 0° N, 69.5° E	Rectangular	F-00N070	MG0009
3. 57.5° S, 165° E	Rectangular to labyrinthic	C1-60S153	MG0031
4. 8.5° S, 87° E	Labyrinthic	F-60S164	MG0063
5. 41.5° N, 261.5° E	Labyrinthic	F-10S087	MG0010
6. 33° N, 268.5° E	Labyrinthic	C1-30N261	MG0040
7. 19° S, 196° E	Rectangular to labyrinthic	C1-30N261	MG0040
8. 68.5° S, 1° E	Labyrinthic	C1-15S197	MG0033
9. 15° S, 86° E	Labyrinthic	C1-75S023	MG0054
10. 56° N, 204.5° E	Labyrinthic	C1-15S077	MG0019
11. 16° S, 57° E	Labyrinthic	F-55N208	MG0028
12. 5° S, 301° E	Pitted or irregular	C1-15S060	MG0016
		C1-00N300	MG0047
		F-05N307	MG0053

**Rectangular Networks.** These form the most integrated valley systems on Venus. The networks are approximately 100 km long and less than a km wide. Rectangular valley networks generally occur in smooth, radar dark plains regions.

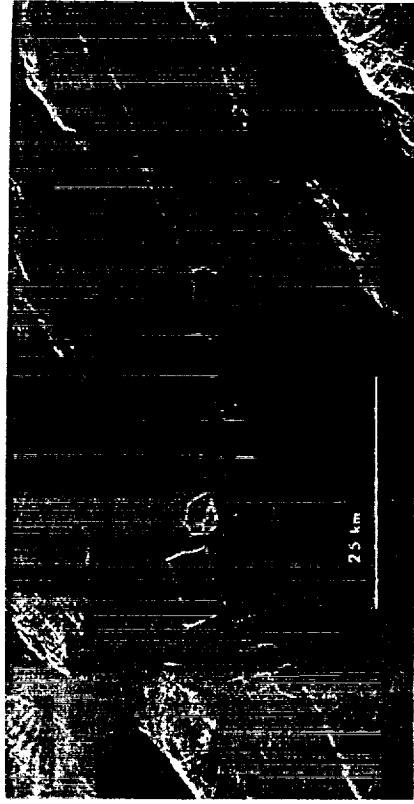


Figure 4. Rectangular valley network located at 2° N, 70.5° E. Image width is approximately 100 km (left-looking radar illumination).

An example is located at 2.1° N, 70.4° E within a narrow 1.5 km wide radar dark plains region (Fig. 4). This network is over 50 km long, less than a km wide and contains at least 15 first-order and 5 second-order tributaries. The right-angled bends of the tributaries and the unusually straight valley segments suggest that the morphological pattern is structurally controlled, although fractures are noticeably absent in the surrounding terrains. Pre-existing (probably subsurface) fractures may have been exploited by subsurface fluid flow (probably of low-viscosity lavas) to create the rectangular networks.

**Labyrinthic Valley Systems.** These are the most common type of valley networks on Venus (see Fig. 14 in Komatsu et al. 1993). Valleys are typically several km wide and a couple hundred of km long, and they appear to have been modified through wall collapse and removal of material along the valley floor. Tributaries have stubby, theater-shaped heads, and the overall pattern is less integrated when compared with rectangular systems. Labyrinthic valley networks are observed within or near tectonically deformed terrains, or near volcanic landforms (such as coronae). The complexity of tectonically deformed terrains precludes clear identification of the relative orientations of valley segments and tectonic structures, although some networks appear to merge with scalloped troughs, which are interpreted to be graben (Solomon et al. 1992). Sinuous rilles have also been observed to connect with labyrinthic valley systems (Komatsu et al. 1993). These morphologic characteristics are similar to those of terrestrial and Martian valleys which were formed or modified by groundwater sapping processes. Lack of significant labyrinthic

valley enlargement suggests that headward erosion along fractures took place at a rate which was several orders of magnitude faster than that at which valley sidewalls could erode. This may have been caused by resistant underlying rock layers, by the permeability of the subsurface layers which contained the eroding fluid, or by the viscosity of the fluid itself.

*Pitted or Irregular Valley Systems.* These are observed in areas of relatively smooth plains containing linear ridges (see Fig. 15 in Komatsu et al. 1993). Pitted or irregular valleys have irregular, scalloped margins which appear to have formed from a series of coalesced pits or scalloped depressions having diameters up to several km. The widest main valley reach is surrounded by a series of larger, loosely organized pits with diameters of several km. Narrower sections of these valleys are bordered by smaller, coalesced pits. These systems may be as long as 300 km and as wide as several tens of km; main valley reaches are typically 50 to 75 km wide. This particular subclass of Venusian valley networks is morphologically similar to areas of thermokarst on Mars (see Figs. 3b and 4b in Gulick et al. 1992b) and to aluvial valleys in permafrost regions on Earth, suggesting that pitted or irregular valley systems on Venus may have formed by an analogous mechanism. The necessary subsurface erosion would have to involve removal of a fluid (lava) or sublimation of a solid. Fields of collapse depressions on Earth are morphologically similar to pitted or irregular valley systems, although these terrestrial pits do not typically coalesce to form valleys (Heacock et al. 1966).

All types of Venusian valley networks are integrated systems of smaller channels (or valleys) whose arrangement appears to have been structurally controlled. They tend to occur in or near tectonically deformed terrains, and they are commonly aligned with fractures or connected to scalloped troughs (graben). The high degree of tributary integration strongly suggests that a fluid (most likely a low-viscosity lava), probably moving in near-surface regions and locally intersecting the surface, formed or modified these networks. Where subsurface fluids encounter pre-existing fractures, surface and/or subsurface erosion is enhanced because fluid flow becomes concentrated along these zones of weakness.

Although the morphology of Venusian valley networks appears to have been structurally controlled, the integrated nature of individual valleys within the systems suggests that fluid flow was also involved in their formation and evolution. Venusian valley networks do not approach the degree of complexity or diversity typically attained by fluvial (water) valleys on either Earth or Mars (Gulick et al. 1992b), but have a higher degree of valley integration than that observed in lunar sinuous rilles. Thus, we propose that the fluid that formed the valleys on Venus had properties which are intermediate between those of water and lunar basaltic lava.

### C. Meander Properties

The range of sinuosities for the measured Venusian channels (Fig. 5) are concentrated between 1.0 and 1.3; published sinuosities of terrestrial rivers

range from 1.0 to 2.3 (Schumm et al. 1972). The relationship between wavelength and width for Venusian channels lies along the same trend as that for terrestrial river meanders (Fig. 6). Wavelength-to-width ratios for Venusian channels vary from 1.99 to 51.68. The similarities between the measured Venusian channels and terrestrial river channels suggests that the channel-forming fluid—which was water on Earth, and (presumably) lava on Venus—behaved in a comparable manner on both planets. Venusian channels with flow margins and canali-type channels tend to have slightly higher  $L/W$  ratios (4.56–26.99 and 3.38–51.68, respectively) for the measured samples (Fig. 6). Although data are limited, terrestrial lava channels-collapsed tubes exhibit a similar trend.

Venusian sinuous rilles tend to be wider for a given wavelength ( $L/W$  ratios in the range 1.99–16.59; Fig. 6) than other channel types on Venus, but have similar meander properties (Fig. 6) to those of lunar sinuous rilles. Experimental lava channels, simulated with hot water flowing on polyethylene glycol (Huppert and Sparks 1985), indicate that meander sinuosity is primarily determined by initial flow discharge (the higher the discharge, the lower the sinuosity). Because the hot water thermally widens and deepens the channel while retaining the original meander sinuosity (Huppert and Sparks 1985),  $L/W$  ratios decrease with time. Because both Venusian and lunar sinuous rilles display unusually low  $L/W$  ratios (Fig. 6), flowing lava may have eroded (through thermal and mechanical processes) both the floors and walls of these channels (Hulme 1973; Komatsu and Baker 1994a).

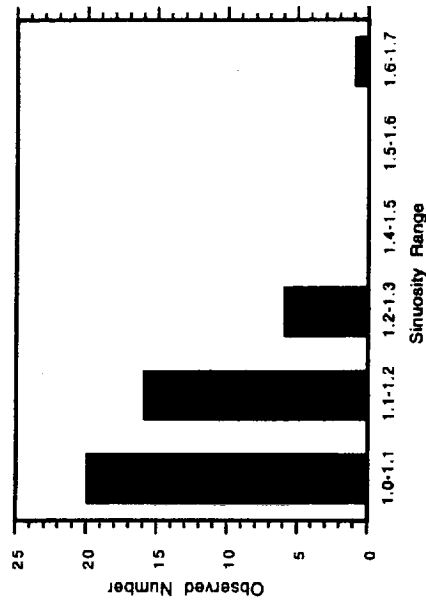


Figure 5. Sinuosity ranges for a representative sample of Venusian channels, illustrating the various classes. Sinuosity is defined as the ratio of the channel length to the length of the meander belt axis (Brice 1964).

Gregg and Greeley 1993). Because terrestrial lava flows remain active for less time than do river channels, the relatively short period of formation may explain why the meanders tend to be less sinuous than in terrestrial rivers.

Specific Venusian channels have multiple wavelength meanders. This phenomenon is observed mostly on sinuous rilles, and it may be caused by either changes in discharge rates or by structural control. At least one canali-type channel (at 33°S, 157.5 to 158.5°E) shows an exceptionally high sinuosity (>1.5). This may indicate a relatively long time scale of flow duration, an attribute consistent with other morphological characteristics of canali, such as their long length and local cut-off bends (Baker et al. 1992).

### III. KALLISTOS VALLIS

While it is not possible to provide a detailed description of the many Venusian channels, we provide here a description of a prominent compound channel, Kallistos Vallis, which illustrates the evidence leading to inferences concerning channel-forming lavas. Kallistos Vallis is a catastrophic lava flood channel, morphologically similar to the "outflow" channels on Mars (Mars Channel Working Group, 1983), though smaller. The channel is over 1200 km long and up to 30 km or more in maximum width. Kallistos Vallis is centered at 50°S, 21°E (Fig. 3). The channel source is a collapse feature on the southwest flank of a broad volcanic complex with gently sloping flanks near the center of Derceto Corona (47°S, 19°E). Derceto Corona is a large, elongate ovoid structure that is bounded by a prominent arcuate ridge belt on its northeast and east sides and a rift valley complex on its west side. This volcanic complex is an elongate feature with broad topographic swells to the northeast and southwest, and a quasi-circular collapsed caldera at its northwest end. The ridge belt is typical of many found at the periphery of several Venusian coronae.

We used detailed geologic mapping to characterize the geologic relations and relative timing of the events which produced Kallistos Vallis. Radar geomorphic units were identified based on morphology, texture, radar brightness, and degree of fracturing using stereo pairs of F-MIDR 50S021 (75 m/pixel, centered at 50°S, 21°E). Both left-looking and right-looking SAR mosaics exist for the Kallistos Vallis region; Cycle 3 SAR (obtained with lower incidence angles than Cycle 1 SAR specifically so that the two sets could be used for stereo geologic mapping) is not available. Despite the opposite illumination geometry in the Cycle 1 and 2 data, stereo viewing is possible for much of the region, because most of the topography is rather gentle. Furthermore, the most interesting reaches of Kallistos Vallis trend east-west, parallel to the look direction, and the incidence angles for the Cycle 1 and 2 images are similar (23° and 25°, respectively) so that the radar-backscatter of nearly horizontal surfaces is comparable. An added benefit from the opposite illumination geometry is that channel walls trending perpendicular to the look direction, if not visible in one view, are usually strong reflectors in the other

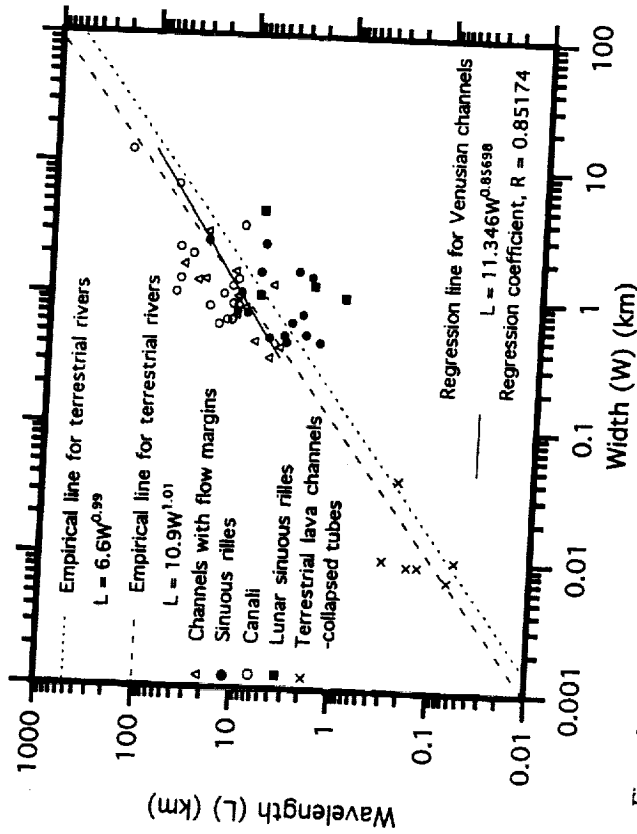


Figure 6. The relation between meander wavelength ( $L$ ) and channel width ( $W$ ) for various Venusian channel types, lunar sinuous rilles, terrestrial lava channels, and collapsed terrestrial lava tubes. Regression line (solid line) is derived for Venusian channels. Two empirical lines,  $L = 6.6W^{0.99}$  and  $L = 10.9W^{1.01}$  (Leopold and Wolman 1960), derived from terrestrial rivers, are shown for comparison.

Studies of terrestrial rivers (Leopold and Wolman 1957; Schumm et al. 1972) and flume experiments (Schumm and Khan 1972) show that meandering occurs within specific ranges of slope and discharge. Theoretical considerations, using energy minimization principles (Chang 1988), also suggest that channel sinuosity is a function of discharge. The morphologic similarity between Venusian channels and terrestrial fluvial channels (Komatsu et al. 1993) suggests that meanders observed in Venusian channels also developed within a limited range of discharge and slope.

On Earth flowing water generates meanders in alluvial sediments by erosion and deposition over some prolonged period ( $\sim 1$  to  $10^2$  yr). For bedrock meanders (or valley meanders), erosion takes even longer. In general, terrestrial lava channels and tubes are constructional and, as a result, meanders develop where channel-forming lava retains its fluidity (see, e.g., Greeley 1974). In contrast to fluvial systems, meander properties of lava channels are determined by the flow characteristics (discharge and slope) during a relatively short-term eruption. Venusian channels presumably generated by flowing lava have been proposed to have formed via construction, erosion, or by a combination of the two (Komatsu et al. 1992a, 1993; Baker et al. 1992;

(Fig. 7). An advantage to "left-right" stereo over "left-left" stereo available for parts of the planet is that topographic resolution is much better because the parallax angle is much larger. At the latitude of Kallistos Vallis, a single pixel of parallax displacement corresponds to approximately 17 m vertical precision. These stereo data coupled with the lower-resolution topography from the radar altimeter make it possible to construct high-precision longitudinal and cross profiles of the channel (Figs. 7, 8, and 9).

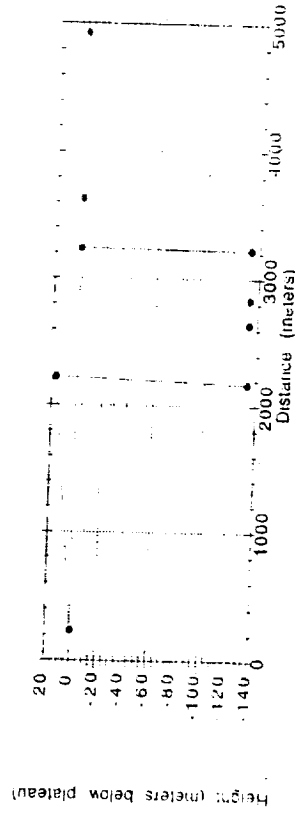
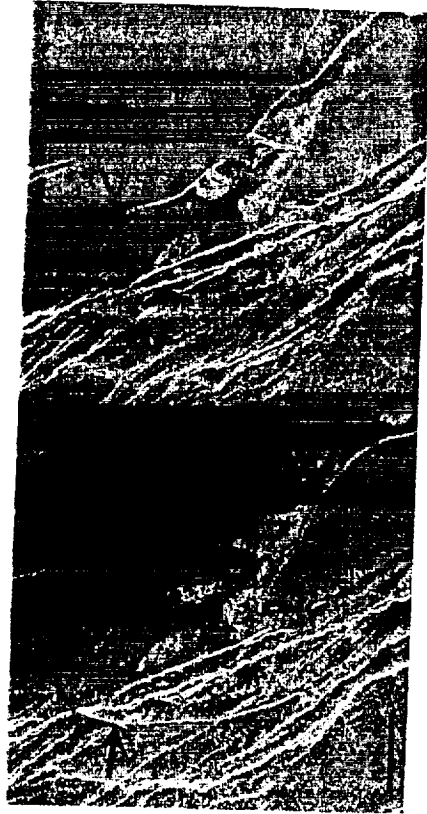


Figure 7. (a) SAR stereo showing where Kallistos Vallis (Fig. 6) spills out of trough reach and begins anastomosing reach. Channel walls are most visible where oriented facing incident radar (arrowed left and right-looking scenes). Cycle 2 (right-looking) image on left, Cycle 1 (left-looking) image on right in this and subsequent figures. (b) Cross-sectional channel profile taken just beyond where the fluid within the trough spilled out. Depth of trough is approximately 145 m.

Parker et al. (1991) divided Kallistos Vallis into three reaches: (1) a collapsed terrain source/trough reach characterized by a deep collapse pit at the head of the system and a deep, structurally controlled trough that contained much of the fluid flow for the first 275 km; (2) a 200-km anastomosing reach exhibiting numerous streamlined islands; and (3) a distributary reach where

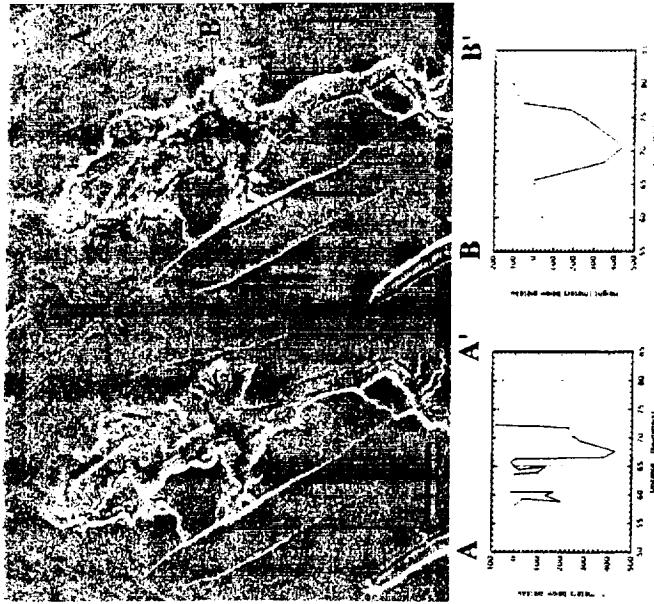


Figure 8. Stereo SAR of collapsed terrain source region for Kallistos Vallis. Depths plotted on right image based on stereo parallax measurements. Note that greatest depth measurement is associated with central, radar-dark floor of structure. Shallower values in conduit to south may be due to infilling of valley by subsequent wall collapse (radar-bright debris aprons from walls).

the flow began to spread across the existing plains to collect finally into a vast, radar-bright lobate deposit over 100,000 km<sup>2</sup> in area. Kallistos Vallis trends south-southeast from the caldera complex for about 400 km, at which point it encounters an elevated unit of fractured terrain that deflected the flow eastward.

The source of Kallistos Vallis is a collapsed region 17.5 km wide by 3.5 km elongate in the northwest direction, parallel to the local structural grain, and over 400 m deep (Baker et al. 1992). This source region is morphologically similar to, though less complex and smaller, than those associated with the well-known Martian outflow channels (Baker 1982; Mars Channel Working Group 1983). Like many of the Martian chaotic terraces, the source of Kallistos Vallis exhibits isolated mesa remnants and founder blocks of the surrounding plains in its interior, a smooth central floor, and prominent aprons of debris at the bases of the cliffs. This trough appears to have been enlarged and deepened where it joins the larger structure, suggesting withdrawal of a subterranean fluid (Fig. 8).

The collapsed terrain source is linked to the trough reach by a 45 km long, incised gorge which appears to have been controlled by local structure

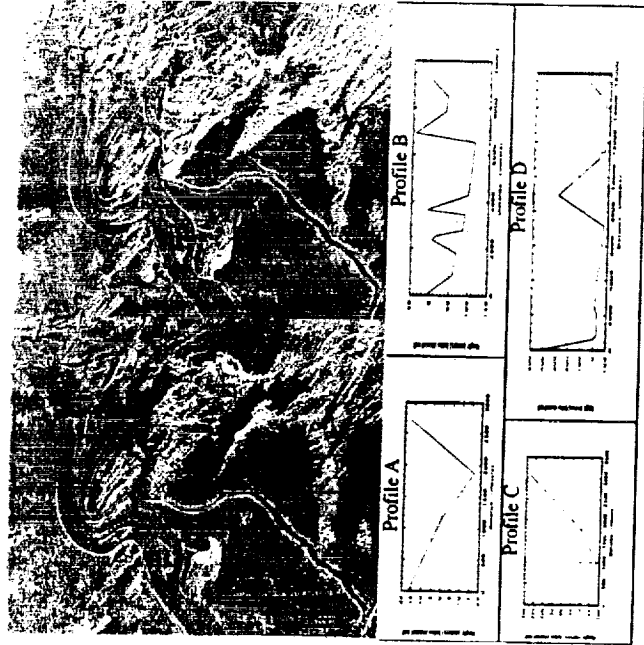


Figure 9. Stereo SAR of spillover from ponded region of Kallistos Vallis at lower end of anastomosing reach. Fractured terrain was breached at two locations: northwest-trending fractured terrain at location of profiles A-C; and north-trending fractured terrain at profile D. Cross-profiles at these locations are indicated at bottom.

and topography. Where the collapse region connects with the trough reach, additional mesa remnants indicate local enlargement of the conduit and trough through collapse. A smaller, relatively shallow collapse trough contained a portion of the flow east of the main trough. There, the fluid spilled out across the plains surface in the form of a shallow, 1.5 km wide sinuous canali (Baker et al. 1992) approximately 175 km long.

The trough reach of Kallistos Vallis appears to be structurally controlled. It is 380 km long, as wide as 4 km, and has a maximum depth of more than 600 m. At its southern end, the trough reach enters the fractured terrain adjacent to the rift valley. Because the fractured terrain is topographically higher than the adjacent plains, the southern end of the trough reach is higher relative to its proximal end.

The anastomosing reach of Kallistos Vallis begins where the trough attains its lowest elevation before crossing onto the fractured terrain. At this point, the trough reach narrows to 1.5 km and shallows to less than 150 m. The channel expands across the plains on either side of the trough to a maximum width of 18 km (Fig. 7). Sixty-five km downstream from this point, the flow leaves the trough completely, having been deflected to the southeast by the elevated fractured terrain. Streamlined islands, consisting largely of plains material, are most abundant in this reach, the largest being 15 km wide and

45 km long. Here, the floor of Kallistos Vallis exhibits a range of radar brightnesses, from bright to dark, probably reflecting variations in roughness on the channel floors on Earth (Fig. 10). At the downstream end of the 300 km long, anastomosing reach, the channel encounters a broken, north-south trending ridge cutting across its path (Fig. 9). Faint channels to either side of the main channel appear to be the remnants of lateral spreading of the flood flow as this ridge temporarily dammed the flow. The main channel within this ponded region was probably formed after the ridge was breached and the lava lake surface dropped. Beyond the ridge barrier, the flood spreads out into a series of distributary channels with radar-bright lobate deposits spreading laterally on either side. The main channel continues for another several hundred km on the depositional plain to the east.



Figure 10. Stereo SAR of upper anastomosing reach of Kallistos Vallis. Post channel faulting has occurred, as evidenced by numerous north trending lineaments left of center and northwest-trending lineament at lower right.

Kallistos Vallis and its terminal deposits are relatively pristine, suggesting that its formation was one of the latest events in the mapped area. Few faults cut the channel, although north-south trending faults cross cut both the channel and its midstream islands, and in the upper anastomosing reach, as well as where the trough cross-cuts the breached ridge. A prominent 135-km-long fault trends northwest, subparallel to the anastomosing reach (Fig. 8). Although this fault appears to cross-cut the channel, it also clearly contained part of the flow through a southern branch for about 60 km, where that branch veered northeastward back toward the main channel. This fault may have been reactivated after the Kallistos Vallis fluid flow event.

IV. GLOBAL DISTRIBUTION AND GEOLOGIC SETTINGS

Venusian channels are widely distributed, but their distribution is not uniform.



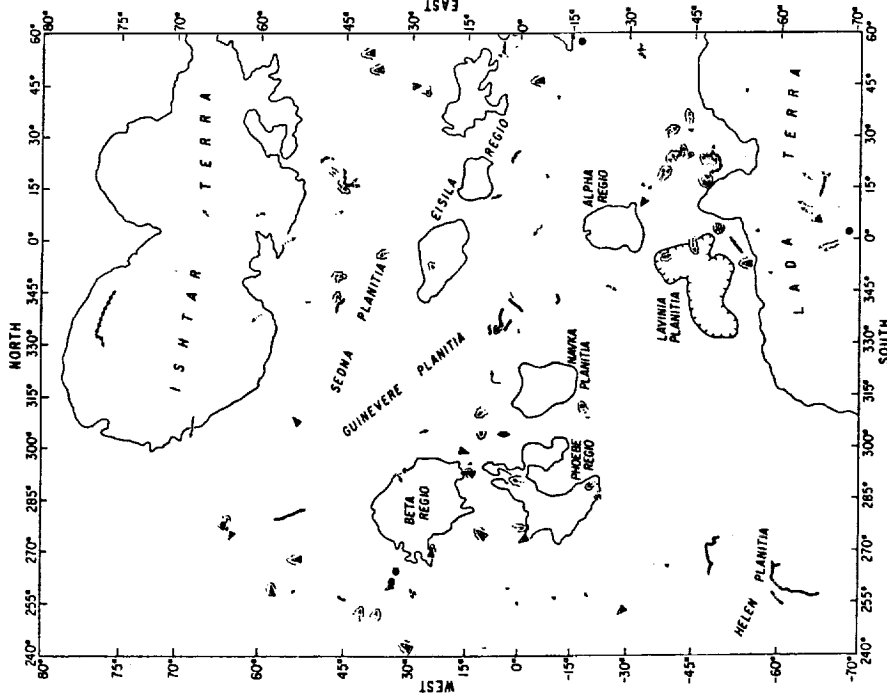
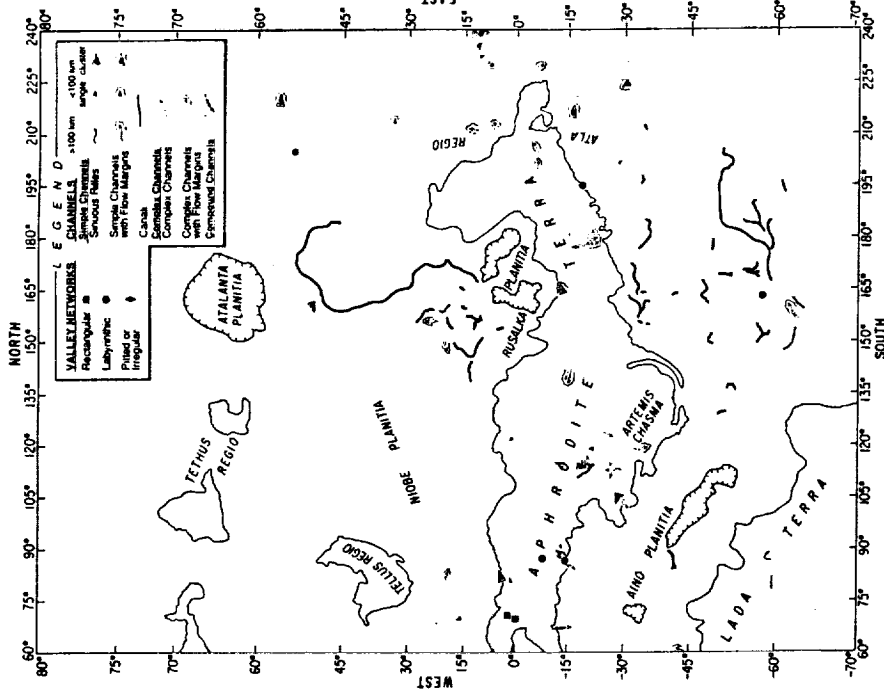


Figure 11. A global distribution of Venusian channels and valleys. The areas north of 80°N and south of 70°S are not shown because of the limited numbers of channels in these small regions (where no valleys are observed). Many simple channels, except for canals, are shorter than 100 km (distinguished by different symbols), while complex channels are generally longer than 100 km (some are clustered, but represented by the longest channels in the map). This may be an observational bias because of image resolution.

Equatorial regions seem to have unusually high channel densities. These areas include highlands, rift and fracture zones associated with large shield volcanoes, coronae, and other volcanic features. These regions contain areas (e.g., the Atla-Beta region) with the highest densities of various volcanic features on the planet (Head et al. 1992). However, as discussed below, there are other regions of low volcanic feature density that have high concentrations of canal-type channels.



Sinuous rilles are widely distributed, but there are several regions of especially high concentration. More than half (39 out of 59, in which clusters of very small sinuous rilles were counted as one) occur on or near coronae, corona-like features or arachnoids, suggesting that channel-forming processes may be closely related to coronae evolution. Flow directions are generally consistent with the regional slope if the rilles occur on highlands.

Some simple channels occur on discernible flow deposits or flow fields with well-defined flow margins. We classify these as simple channels with flow margins. These channels are generally shallow and do not appear to incise into the surrounding terrain. This is consistent with a constructional lava-flow origin (Komatsu and Baker 1992b). Such channels are sinuous, and narrow toward their termini. However, they commonly lack source depressions and do not show the distal shallowing typical of sinuous rilles. We find that simple channels with flow margins are widely distributed (Fig. 11) and that they commonly feed extensive lava flows associated with various volcanic

edifices (e.g., coronae, shield volcanoes, rift and fracture zones). Canali are concentrated in several plains regions, including southern Guinevere Planitia, Helen Planitia, eastern Aino Planitia (southeast of Artemis Chasma), and the plains north of Rusalca Planitia. The channels trend in somewhat random directions, and occur on relatively smooth plains that have a low density of tectonic and volcanic features. Few canali have clearly defined sources or termini. All regions of canali concentration are topographically smooth, leading to a potential observational bias, whereby we might more easily recognize canali in plains than in other geologic units. For other geologic units, the channels might be destroyed by subsequent geologic processes, or they might be more difficult to discern. However, not all plains have a high concentration of canali. Small-scale canali may be found in future analysis of increased-resolution images. Nevertheless, the fact that canali larger than certain scale are observed only in some specific plains suggests that those plains favor their formation. All canali are more or less modified by subsequent tectonism and/or volcanism, indicating that their formation was not geologically recent.

Complex channels with flow margins are widely distributed (Fig. 11). These channels feed extensive lava flows that are associated with various volcanic edifices (e.g., coronae, shield volcanoes, rift and fracture zones). Networks are rare. They are observed in the highlands, particularly in Aphrodite Terra. They are sometimes closely associated with corona, corona-like features or arachnoids.

## V. GENETIC PROCESSES

### A. Canali

Canali-type channels are typically longer than 500 km, and the longest ones are as long as 6800 km (Komatsu et al. 1993). These channels are unique for their nearly constant width along their entire length. Cross-sections of possible canali structures are summarized in Fig. 12. Unlike typical lava channels on Earth, most canali lack obvious levees or lateral flow deposits, although these are observed locally (Komatsu et al. 1992a; Gregg and Greeley 1993). Some canali have features which resemble those of terrestrial fluvial channels, such as oxbows (see Fig. 5b in Baker et al. 1992), point-bars, lateral migration of meanders (see Figs. 1 and 2 in Kargel et al. 1994), highly sinuous reaches (see Fig. 6b in Komatsu et al. 1993), fan-shaped terminal deposits (see Fig. 5a in Baker et al. 1992), and deltas (see Fig. 6 in Kargel et al. 1994). The analogy between canali and fluvial channels implies erosional processes for the formation of canali. However, Komatsu et al. (1992a) and Gregg and Greeley (1993) presented some arguments against erosional processes by low viscosity silicate lavas, including mafic alkaline lavas and ultramafic lavas, as a primary canali formation mechanism. It is unlikely that silicate lavas (such as basalt or komatiite) would be able to maintain turbulence along the observed canali lengths—they would cool and become too viscous—and

turbulence greatly enhances the processes of thermal and mechanical erosion. Thus, the ability of a lava flow to erode decreases with increasing distance from the vent, implying that erosional channels should shallow distally. This distal shallowing is not observed in canali.

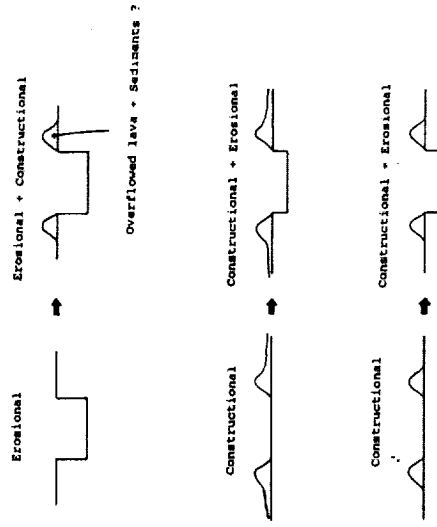


Figure 12. Cross-sections of hypothetical canali structures based on whether they were formed primarily by constructional or by erosion.

The constructional origin of canali has been also proposed and discussed (Komatsu et al. 1992a; Gregg and Greeley 1993). Mafic, including mafic alkaline, and ultramafic, lavas can flow the required distances beneath an insulating crust (Komatsu et al. 1992a). The thermophysical properties of the Venusian atmosphere cause it to cool efficiently the surface of a mafic lava flow via convection, enhancing the growth of a lava crust and promoting longer flows (Gregg and Greeley 1993). Gregg and Greeley (1993) suggested that thermal erosion on Venus is less efficient due to the smaller temperature differences between the lava and the ground rock on Venus than on Earth. Hence, they concluded that the canali are most likely the product of mechanical or constructional processes, but this does not preclude the formation of fluvial-like morphologies by the lava while it is still fluid. Alternatively, canali may be collapsed lava tubes; roofing over of the channel would thermally insulate the lava and decrease the cooling range. Assuming that the roof of a lava tube can be approximated as an unsupported beam, Oberbeck et al. (1969) proposed that the maximum width of uncollapsed, unsupported terrestrial basaltic lava tubes is  $\sim 30$  m. Maximum lava tube width on Venus would be similar, because gravitational acceleration is only slightly lower. Without lava supporting the solid crust, channels greater than 30 m in width would be unable to sustain a crustal roof, and typical canali are much wider than 30 m. Thus, if canali are collapsed lava tubes, their floors should be littered with collapsed roof segments, and there is no clear evidence for this. However, it

is also possible that some canali may have roofed reaches (Bussey and Guest 1992). The general absence of levees or lateral flow deposits also argues against a constructional origin for canali (Komatsu et al. 1992a, 1993). It is possible that the levees or lateral flow deposits are not observed because the channel-forming lava had a very low yield strength, resulting in a very narrow levee. Alternatively, a fluid lava may generate levees or lateral deposits which are too smooth to be distinguished from the background plains on Magellan imagery. Finally, degradation processes may have obliterated the levees or lateral flow deposits. It is possible that canali may have been formed by lavas which are exotic in composition (by terrestrial standards), and both sulfur and carbonate flows have been proposed (Komatsu et al. 1992a; Baker et al. 1992; Kargel et al. 1994; Treiman 1994; Gregg and Greeley 1994). Sulfur's melting temperature is below the surface temperature of Venus at ambient conditions, and thus, would never solidify (Fig. 13). The viscosity of sulfur under Venus surface conditions is comparable to that of liquid water on Earth. Thus, although sulfur cannot thermally erode silicate ground rock, sulfur flows should be able to travel great distances even at relatively low discharge rates. Sulfur flows could possibly construct channel banks by deposition of eroded materials, similar to terrestrial rivers. However, the low humidity of sulfur in the Venusian atmosphere causes liquid sulfur to evaporate rapidly upon exposure to the surface. Alkali-rich carbonates have melting points comparable to or slightly greater than the Venus ambient temperatures, potentially allowing considerable travel distance and mechanical erosional capacity (Fig. 13). Furthermore, carbonates have melting points lower than those of silicate lavas, and viscosities which are orders of magnitude lower. Like sulfur flows, carbonate lavas could not thermally erode silicate materials, but should be able to travel great distances before solidifying, even with low flow rates. Because carbonate lavas should eventually solidify at Venusian surface conditions, they may form a channel constructionally. However, the low viscosity of carbonate should promote mechanical erosion. Although the  $\text{CO}_2$  pressure of the Venusian atmosphere is near carbonate saturation, there is some evidence that solid carbonate is unstable at Venusian surface conditions, and may eventually sublime.

Even though sulfur and carbonate are rheologically satisfactory, these lavas are only generated in small volumes on Earth today, and it is difficult to explain how they could be produced in such quantities on Venus. The dimensions of the longest canali-type channel (6800 km long by 1 km wide by 20 m deep) indicates that the total amount of sulfur lava required to scour the channel is about  $10^{12} \text{ m}^3$ , assuming the ratio of lava to eroded material is 10. Because carbonate lavas are capable of forming constructional channels on Venus, they may be able to form a similar channel with less lava; however, the required volumes will still be much larger than observed carbonate eruptive volumes on Earth. No known terrestrial examples of sulfur and carbonate volcanism match this scale. If canali were formed by such exotic lavas, the erupted volumes would indeed be unique among the terrestrial planets.

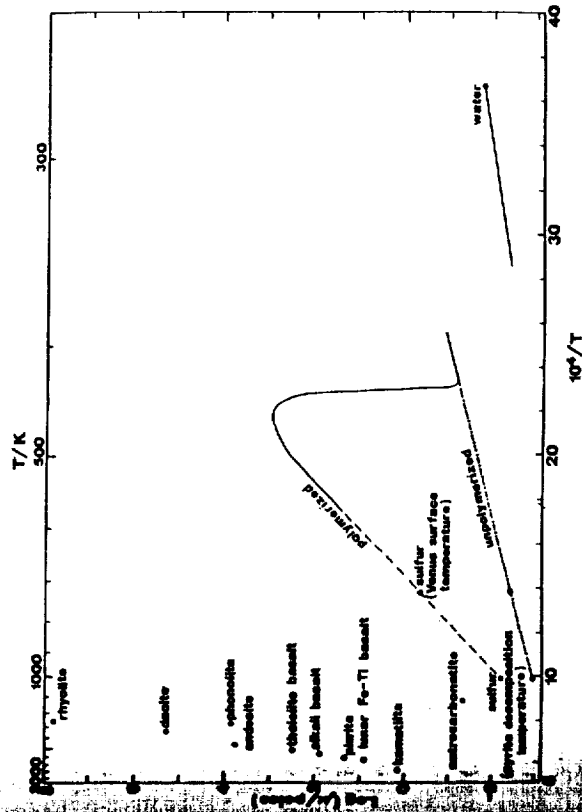


Figure 13. Viscosities and eruption temperatures of possible Venusian lavas.

## B. Sinuous Rilles

Sinuous rilles received their name because of their close resemblance to lunar sinuous rilles. Like the latter, Venusian sinuous rilles narrow and shallow downstream, originate from collapse pits, have sections as deep as several hundreds meters, and do not normally have observable levees or lateral flow deposits. Various origins have been proposed for the lunar sinuous rilles, including lava drainage channels (Strom 1965), collapsed lava tubes (Oberbeck et al. 1969; Greeley 1971) and thermally eroded lava drainage channels (Hulme 1973, 1982; Carr 1974).

Venusian sinuous rilles were most likely formed as a high-temperature, low-viscosity lava thermally eroded the underlying material during a high-discharge-rate, long-duration eruption. Sinuous rille depths, obtained from foreshortening relations and stereo images, may be too great to have been formed by simple lava drainage or construction processes (Komatsu et al. 1993), and thus may be the result of thermal erosion processes. The meander characteristics of Venusian and lunar sinuous rilles are distinct from those of canali and typical terrestrial lava channels (Fig. 6) (Komatsu and Baker 1994a; Kargel et al. 1994). These differences may be due to the involvement of erosional processes, particularly thermal erosion, in the genesis of sinuous rilles. Because more than half of the Venusian sinuous rilles are associated with coronae, corona volcanism may have contributed to the conditions for the channel formation (Komatsu et al. 1993).

The lunar sinuous rilles which are most similar in morphology to Venusian sinuous rilles are those that most probably formed by lava with high Fe-Ti content in comparison with terrestrial tholeiitic basalt (Murase and McBirney 1970). High Fe-Ti basalt has a higher melting temperature (and presumably higher eruption temperature) and lower viscosity than typical tholeiitic (Murase and McBirney 1970). The one-dimensional thermal erosion rate  $E$  is expressed by the equation (Huppert and Sparks 1985)

$$E = h(T_l - T_{mg}) / \rho_g [C_g(T_{mg} - T_0) + L_g] \quad (1)$$

in which  $h$  is the empirical heat transfer coefficient,  $T_l$  is lava temperature,  $T_{mg}$  is ground melting temperature,  $\rho_g$  is a ground density,  $C_g$  is ground heat capacity,  $T_0$  is initial ground temperature, and  $L_g$  is ground latent heat of fusion. The empirically determined heat transfer coefficient  $h$  (for Earth) is (Huppert and Sparks 1985)

$$h = 0.02k/d Pr^{0.4} Re^{0.8} \quad (2)$$

in which  $k$  is a thermal conductivity;  $Pr$  is the Prandtl number as a function of dynamic viscosity  $\eta$ ; specific heat  $C$  and thermal conductivity of the lava (given below);  $Re$  is the Reynolds number determined by two-dimensional discharge rate ( $Q_{2D}$ ) and kinematic viscosity of the lava  $\nu$ ; and  $d$  is the thickness of the flow and a function of discharge rate. These variables are related as follows:

$$Pr = \eta C / k \quad (3)$$

$$Re = Q_{2D} / \nu \quad (4)$$

As shown in Eqs. (1), (2), (3), and (4), the thermal erosion rate is controlled by lava temperature and viscosity when other conditions are similar. Figure 14 illustrates erosion rate estimates for various lava types incising tholeiitic ground material. For tholeiitic lava to erode tholeiitic ground efficiently, the lava must be superheated or the flow duration must be very prolonged. Superheating can happen if the magma ascends through the crust without significant heat loss, or if the basaltic crust is heated from below by hotter ultramafic magma from a mantle plume. Unless superheated, tholeiitic lava might construct sinuous rilles, but it could not thermally deepen and widen them to a major extent. Lunar basalt, high-MgO lavas, such as komatiite and picrite, and mafic alkaline lava all have more capability for efficient thermal erosion than does tholeiitic basalt, because of high eruption temperatures and low viscosities. These factors will lead to high thermal erosion rates, particularly when the lava flows across ground materials of relatively low melting temperature (Huppert and Sparks 1985).

We conclude that the origin of Venusian sinuous rilles is a problem that can be resolved by direct analogy to the origin of lunar sinuous rilles. Highly prolonged and/or very hot lavas are required to achieve considerable thermal

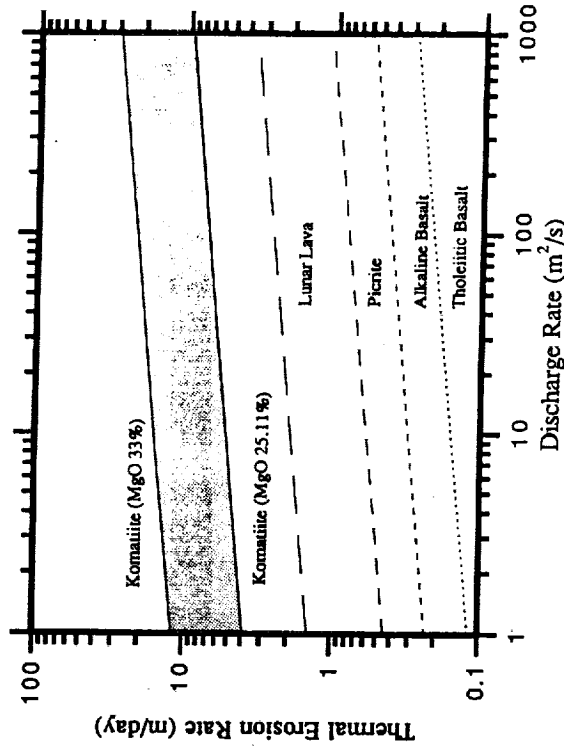


Figure 14. Thermal erosion rates of tholeiitic ground rock on Venus by various lava compositions with various flow rates. The Chezy equation was used to relate flow thickness and discharge rate (Komatsu et al. 1992a). Lavas were assumed to erupt at their respective temperatures, and the ground rock was assumed to have a melting temperature of 1270°C. For simplicity, thermal conductivity and specific heat were assumed to be  $1 \text{ W m}^{-1} \text{ K}^{-1}$  and  $730 \text{ J kg}^{-1} \text{ K}^{-1}$ , respectively, for all rock types. Other parameters, liquidus temperature, viscosity, density and latent heat of fusion for the ground material were derived from Murase and McBirney (1970, 1973), Ryerson et al. (1988), and Huppert and Sparks (1985). For the komatiite, a liquidus temperature range of 1500 to 1650°C (MgO content 25.11–33%) was chosen (erosion rate range is shown by the dotted area). Lunar lava is represented by a mare basalt collected during the Apollo 11 mission. Picrite is represented by a sample collected at the Kilauea Iki Lava Lake. Alkaline basalt is represented by Galapagos Island Basalt. Tholeiite is represented by Columbia River Plateau Basalt within an assumed melting temperature of 1300°C. For simplicity, all flows are assumed to be turbulent.

erosion. The canali, in contrast, have morphologies that are unique for lava channels. Their genesis requires highly fluid lavas, erupted at sustained, high discharges. Unusually low viscosities are required to explain fluvial-like features. Only the most fluid of silicate lavas would be candidates. Carbonatite and sulfur lavas are also possibilities, though their abundance would be highly unusual for terrestrial planetary geochemistry.

### C. Genesis of Kallistos Vallis

The compound channel Kallistos Vallis deserves special attention because its morphology indicates massive outpourings of low-viscosity fluid (Baker et al. 1992; Parker et al. 1995). This channel is wide, originates from a collapsed pit, and has braided reaches. These characteristics are typical of Martian

outflow channels, which implies the channels origin by high discharge flows. Kallistos Vallis forms radar bright levees/lateral flow deposits at its terminus, and this indicates that the channel was formed by lava.

The channel seems to have been formed by highly turbulent flow as suggested by the shapes of streamlined, probably erosional landforms (Fig. 3). For highly turbulent flow, the velocity can be approximated by a Chezy equation of the form

$$v = C(\alpha)^{1/2} \quad (5)$$

where  $C$  is the Chezy coefficient ( $C = 1/\pi(d)^{1/6}$ ,  $n$  is the Manning coefficient),  $d$  is flow thickness, and slope  $\alpha = 0.0005$ . Because  $C$  is proportional to  $g^{1/2}$  (where Venus gravity  $g_V$  is  $8.87 \text{ m s}^{-2}$ ), the Manning coefficient for Venus ( $n_V$ ) can be related to the empirical terrestrial Manning coefficient ( $n_E$ ), by the equation  $n_V = n_E(g_E/g_V)^{1/2} = 1.05n_E$ . This correction is very small compared with the range of possible Manning coefficients. Note that Eq. (5) ignores the viscosity factors that usually dominate in lava-flow mechanics. However, we cannot conceive of how flows with appreciable viscous effects could generate the landforms observed for Kallistos, so we are presuming highly turbulent flows in the calculations to follow.

Using Eq. (5) we calculate the velocities for a range of flow thicknesses ( $d = 1, 10, 100 \text{ m}$ ). The range of discharge rates (three-dimensional) is estimated as  $5 \times 10^7$  to  $5 \times 10^9 \text{ m}^3 \text{ s}^{-1}$  ( $d = 1-100 \text{ m}$  and  $n_V = 0.015-0.150$ ), because the range of width is about 3 to 15 km. A range of  $d = 1$  to 100 m was chosen, assuming that the flow thickness was less than the depth of the channel. In the case of terrestrial catastrophic flood channels, the high water marks come close to the edge of the banks. If the morphology of the Kallistos Vallis is a result of flow processes similar to those of catastrophic flood channels on Earth, we can assume that the maximum flow thickness was equal to the depth of the channel, and this gives the peak discharge rates.

If lava solidified on the channel floor, the depth may not really represent the flow thickness. Indeed, the depth/width ratio of the channel is much smaller than is typical for terrestrial and Martian outflow channels. Moreover, the slope may have been significantly different at the time of formation, because the draining of a large quantity of lava could have caused a subsidence of the region. Our estimate is subject to the above limitations. The estimated discharge or effusion rate is comparable to those for some maximum-scale volcanic and fluvial processes in the solar system (Table II).

We also estimated the range of power per unit area  $W$  of the flows. The flow power is given by the formula

$$W = \gamma Q\alpha/w \quad (6)$$

where  $\gamma = \rho g$  is the specific weight of the fluid ( $23949 \text{ N m}^{-3}$  for silicate lava) and  $w$  is the width of the channel. For a flow 10 m thick, and slope  $\alpha = 0.0005$ , the range of  $W$  is  $83 \text{ W m}^{-2}$  (at  $n_V = 0.15$ ) to  $830 \text{ W m}^{-2}$  (at  $n_V = 0.015$ ). This range of  $W$  is equivalent to powers of some terrestrial floods (Baker and

Discharge Rates of Major Volcanic and Fluvial Events in the Solar System

References	Three-dimensional	Two-dimensional	Volcanic process
Hulme and Fieder 1977 Head and Wilson 1980	$10^4$ to $10^6 \text{ m}^3 \text{ s}^{-1}$ $10^7$ to $6 \times 10^8 \text{ kg s}^{-1}$		Lunar channel forming event
Head and Wilson 1986 Hulme 1974	$10^4$ to $10^5 \text{ m}^3 \text{ s}^{-1}$ $8 \times 10^4 \text{ m}^3 \text{ s}^{-1}$		Lunar flood basalt event
Swanson et al. 1975		$1 \text{ km}^3 \text{ day}^{-1} \text{ km}^{-1}$ ( $11.5 \text{ m}^2 \text{ s}^{-1}$ )	Terrestrial flood basalt event
Huppert et al. 1984		$1$ to $10^2 \text{ m}^2 \text{ s}^{-1}$	Terrestrial komatiite flow
			Fluvial Process
Baker 1982	$10^5$ to $10^8 \text{ m}^3 \text{ s}^{-1}$		Martian outflow channels
Baker 1982	$3 \times 10^4 \text{ m}^3 \text{ s}^{-1}$		Mississippi River
Baker 1982	$10^5$ to $10^7 \text{ m}^3 \text{ s}^{-1}$		Missoula Floods

TABLE II

Costa 1987). This large power is strongly suggestive of mechanical erosion, which may have played a very important role in the formation of this channel.

#### D. Valley Networks

Because the Venusian valley networks are morphologically similar to terrestrial and Martian valleys modified through ground-water sapping processes (Gulick et al. 1991; Komatsu et al. 1996), a lava-sapping process was proposed for their origin (Komatsu et al. 1992b, 1996). Although lava sapping is not known on Earth, the process is thought to be somewhat analogous to ground-water sapping with low-viscosity lava as the eroding fluid. In this hypothetical scenario, outflow of low viscosity lava from the subsurface would remove substrate, resulting in collapse of overlying material and subsequent enlargement of existing valleys in a manner similar to ground-water sapping on Earth and Mars (Baker et al. 1990). Low viscosity lava with properties which approach that of water would flow preferentially along buried fracture systems. High-temperature, low-viscosity silicate lavas (such as basalt or komatiite) would warm the fracture walls, possibly resulting in melting or mechanical plucking of wall material and its subsequent incorporation into the flowing lava. This process of thermal erosion (see, e.g., Hulme 1973; Carr 1974) would create a self-enhancing relation; thermal expansion of the fractures allows more lava to flow through, which in turn increases the rate of thermal expansion. The process would cease either when subsurface outflow of lava was insufficient to maintain sapping or when lava viscosity increased due to cooling.

Carbonatite and sulfur lavas are attractive candidates for the sapping fluid, because of their low viscosities and melting temperatures (see discussion in Sec. V). Although, these fluids cannot thermally erode silicate host rocks, they can physically remove unconsolidated material. Exotic lavas are especially favorable for forming the pitted or irregular valley networks where sulfur may have evaporated in a manner similar to sublimating ice in thermokarst landforms on Earth and Mars. Solidified carbonate may sublime for present Venus surface conditions (Kargel et al. 1994). Carbonatite and sulfur flows have appropriate rheologies to have formed the Venusian sapping valleys. However, as with the Venusian channels, the necessary volumes of these magmas are problematic. In terrestrial sapping processes, the amount of water required to erode valleys in the Colorado Plateau would be on the order of  $10^2$  (if the ground is unconsolidated sediments) to  $10^5$  (if the ground rock is consolidated rocks) times more than the amount of eroded material (Howard et al. 1988). Similarly, Gulick (1993) and Gulick and Baker (1993) concluded that the ratios of the amount of water required to erode valleys in the Hawaiian volcanic terrains is approximately 3000:1. Assuming that low-viscosity lavas on Venus can mechanically and chemically erode their host rock in a manner similar to that of terrestrial groundwater, the volumes of magma required to form the Venusian valley networks can be estimated. For example, using a volume of  $\sim 10^{10}$  to  $10^{11}$  m<sup>3</sup> for the valley networks at 57.5°S, 166°E, the

required lava volume would be  $\sim 10^{12}$  to  $10^{16}$  m<sup>3</sup>. As discussed in the section on channel genesis, the production of such large volumes of exotic lava has not been documented on Earth. Thus, it is difficult to understand the generation of these amounts of carbonate or sulfur flows on Venus.

#### VI. DEFORMATION OF LONGITUDINAL PROFILES

The longest canali-type channel, Baltis Vallis (previously named Hildir Fossa), is located west of Atla Regio (Fig. 15). The channel longitudinal profile (Fig. 16) is highly undulatory. The undulations in the profile occur at multiple superimposed scales implying that the deformation pattern is hierarchical (Komatsu and Baker 1994b). Because the channels are sinuous, scales of the profile undulations do not precisely correlate exactly with the linear scales of tectonic deformation observed in the surrounding plains. Thus, listed scales of deformation are approximate and relative to the sinuous trend of the datum provided by the channel path. In Fig. 16 at least two scales are observed: a smaller one at a few hundred km and a larger one at a few thousand km.

We hypothesize that these two wavelengths represent the characteristic modes of tectonic deformation in the plains regions (Figs. 16 and 17). The long scales ( $\sim 10^3$  km) correspond to the characteristic scales of basin structures, and the short scales ( $\sim 10^2$  km) correspond most closely to belts of compressional ridges visible on the SAR imagery (Fig. 15). Note that on a three-dimensional perspective of the topography (Fig. 17), a complex of quasi-circular domes and basins occurs at  $\sim 10^2$ -km scale, which corresponds to the ridge belts and intervening plains.

Not appearing on the regional-scale SAR scene (Fig. 15) are numerous wrinkle ridges (average spacing 20–40 km) with multiple orientations which are nearly ubiquitous on the Venusian plains (McGill 1993). These are not crucial in the topographic profiles (Fig. 16) because of the large spacing of altimetric sampling and the large area of the altimetric footprint. Wrinkle ridge formation postdates the emplacement of Baltis Vallis in this region, although the canali-type channel is superposed by more recent lavas. Highlands probably already existed at the time of channel formation because the channel seems to avoid the northern arms of Atla Regio (Fig. 15). This channel is postdated by lava flows, impact cratering and various episodes of tectonic deformation, as indicated by the disruptions in the channel reaches (Fig. 15).

The second longest Venusian channel is located in eastern Aino Planitia (Fig. 18). Undulations in this channel's longitudinal profile also occur at multiple scales (Fig. 19). The long scale ( $\sim 10^3$  km) does not obviously correspond with any geologic feature in the SAR image. However, at a more regional scale, this concave undulation can be related to an elongate basin oriented transverse to the channel's flow direction (approximately east two-third of the profile is traversing the basin). The short-scale undulations ( $\sim 10^2$  km) can be associated with belts of compressional ridges that parallel the long axes of the basin. The north-trending lineaments in Fig. 18 are wrinkle



Figure 15. Atla Regio, plains and Baltis Vallis (highlighted). The image covers latitude 9 to 53 N and longitude 150 to 200 E. Longitudinal topographic profile is derived between A and A'. The northern reaches of the channel avoid the northern rim of Atla Regio, indicating that channel formation postdates this highland region. The channel is disrupted by lava flows, impact cratering and various episodes of tectonic deformation.

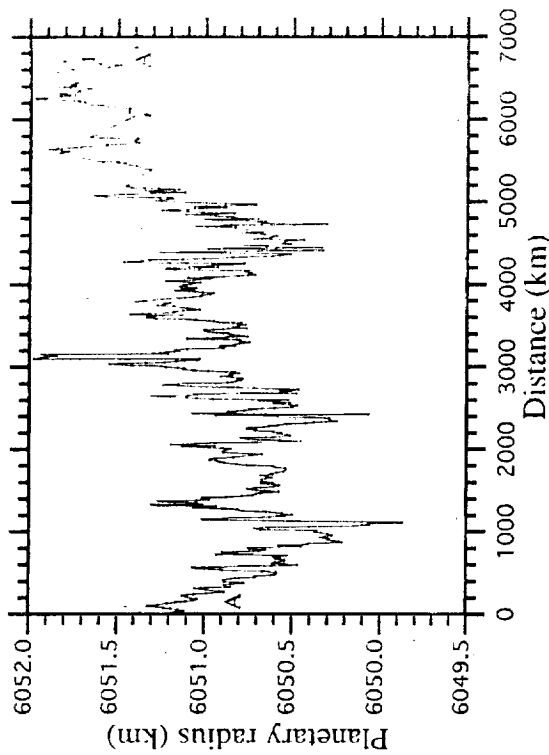


Figure 16. Longitudinal profile of Baltis Vallis.

ridges with an average spacing of 20 to 40 km. As mentioned previously, wrinkle ridges do not appear in the topographic profile. Some wrinkle ridges may have formed concurrently with canals, as suggested by locally diverted channel directions. The tectonic explanation for profile undulations seems to be post-channel downwarping of the basin concurrently with formation of compressive ridge belts and wrinkle ridges.

Sinuuous rilles also show signs of deformation in their longitudinal profiles. Figure 20 illustrates a sinuous rille which trends downhill. The channel may have been deformed, but this deformation was not extensive enough to reverse the trend. Figure 21 illustrates an example of upwardly deformed sinuous rille. Among the sinuous rilles investigated, all of them are less than 500 km and most of them are less than 150 km (Fig. 22), indicating that the deformation scales recorded on sinuous rilles are much smaller than for canals.

On Earth, where a river crosses a region of slow, continuous deformation, the river adjusts its bed to the deformation to maintain a continuous graded profile (Mackin 1948). The profile is maintained through time by deposition at the downwarps and by incision at upwarps. The classic example is the Colorado River, which maintained its grade across the rising domal uplift of the Colorado Plateau (Powell 1875; Hunt 1969). On Venus, canals probably formed in a relatively short time interval at the end of the major phase of volcanic plains emplacement (Komatsu et al. 1993). The original profiles, while

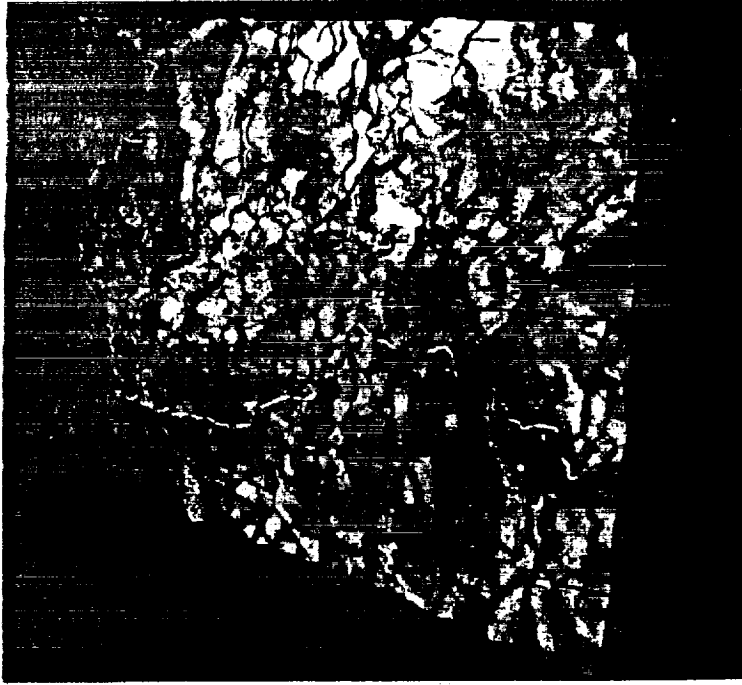


Figure 17. Three-dimensional perspective of Atla Regio and Baltis Vallis (highlighted).

not horizontal, probably reflected a rather uniform gradient of topography that was followed by gravity-driven, sustained flows of lava (Komatsu et al. 1992a, 1993). Thus, all cumulative post-channel, long-acting tectonic warping is reflected in the profiles. On Earth, active rivers would have maintained grade across such warpings, and erosion of uplands or filling of basins would have masked their surficial expression.

On Venus, the multiple deformational scales recorded in canali longitudinal profiles fall into clearly distinct size classes. This scaling hierarchy suggests that each deformational scale may be associated with a different tectonic process of the Venusian interior. Solomon et al. (1992) recognized multiple scales of tectonic features and pointed out that 10- to 30-km-scale structures can be attributed to the response of a strong upper crustal layer (Zuber and Parmentier 1990). In contrast, the deformation of a strong mantle layer can account for tectonic features with characteristic scales of a few hundred to a few thousand km (Zuber and Parmentier 1990), particularly where these scales can be identified in the long-wavelength gravity as well as the topography (Kiefer et al. 1986). This large scale is hypothesized to be dominated by

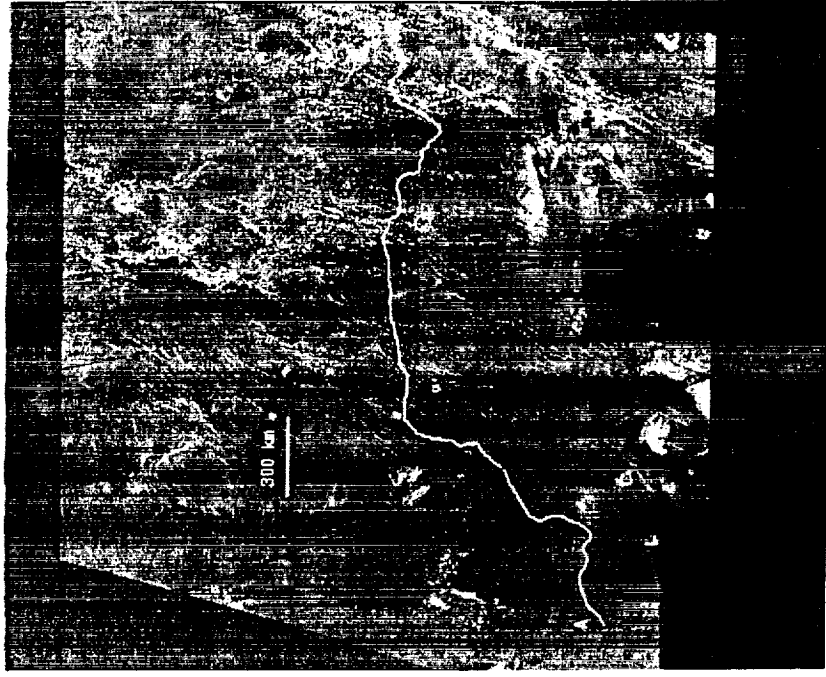


Figure 18. A canali-type channel in the eastern Atla Planitia (highlighted). The image covers latitude 40 to 63°S and longitude 175 to 208°E. Longitudinal topographic profile was derived between A and A'.

mantle convection and its associated dynamic stresses and heat transport. The thousand-km-scale features include broad rises and basins in plains regions. It has been suggested that plains are sites of mantle downwelling (Zuber 1990; Phillips et al. 1991). Bindshadler et al. (1992) identified Atalanta Planitia and Lavinia Planitia as surface expressions of young mantle coldspots or regions of mantle downwelling. Longitudinal profiles, particularly for the longest and second longest channels (Figs. 16 and 19) clearly indicate formation of basins and associated compressional ridge belts after channel formation. The scale of a few km and less involves either internal deformation of the upper crust or tectonic disruption of a thin surficial layer decoupled thermally or mechanically from the remainder of the otherwise strong upper layer (Solomon et al. 1992).

The time sequence derived from the stratigraphic relationships indicates



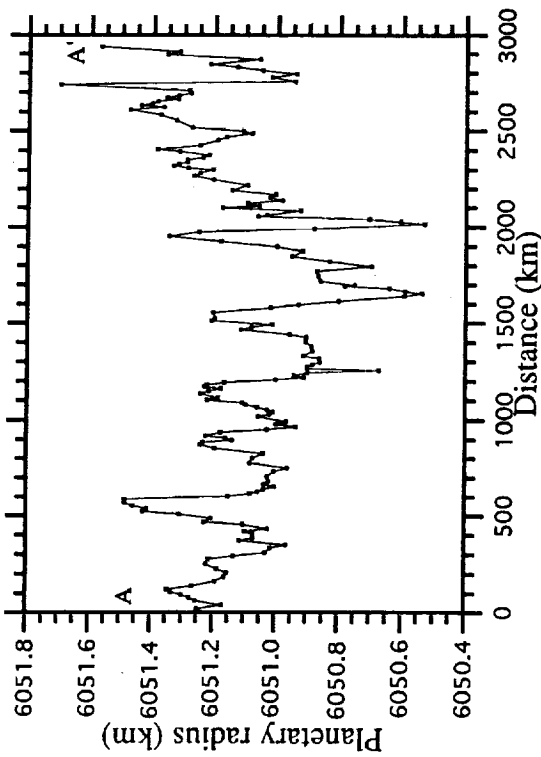


Figure 19. Longitudinal profile of canali-type channel in eastern Aino Planitia (Fig. 18).

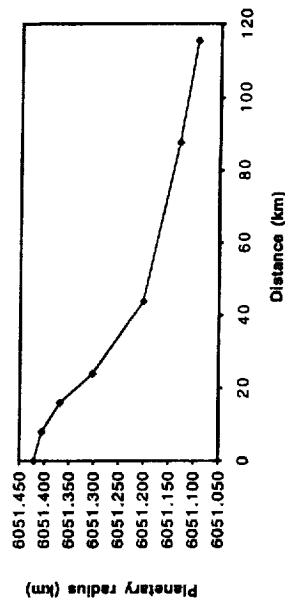


Figure 20. Longitudinal profile of a sinuous rille at 0°N, 255°E. This channel trends downhill. Any deformation that may have occurred did not deform the profile to trend uphill.

that canali are among the younger landforms on the plains, and that their formation is closely related to the last phases of extensive plains volcanism, possibly induced by the hypothesized global resurfacing event (Schaber et al. 1992). The multiple scales of plains deformation recorded in canali profile undulations therefore reflect the various deformation processes of the Venusian interior that operated after the major plains resurfacing epoch (Komatsu and Baker 1994b). This event is estimated to have occurred at approximately 190 to 600 Myr (Strom et al. 1994).

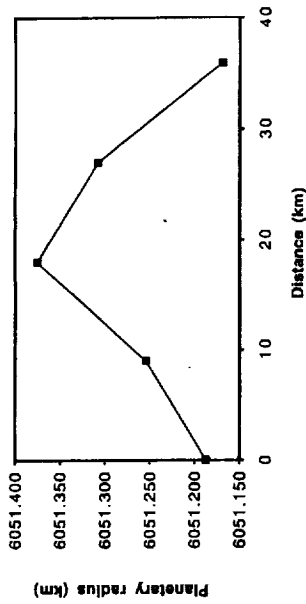


Figure 21. Longitudinal profile of a sinuous rille at 1°N, 259°E. This channel has an upwardly deformed profile. This deformation may be caused by tectonic activity of nearby volcanic dome.

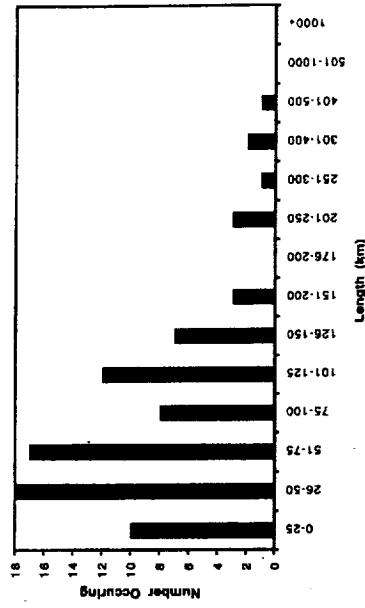


Figure 22. Length distribution of sinuous rilles.

### VII. CONCLUSIONS

More than 200 Venusian channels and valleys are recognized in a global context. Some channels with associated flow deposits are similar in appearance to terrestrial lava channels. Sinuous rilles, similar in morphology to lunar sinuous rilles, most likely formed through erosion processes in high-effusion-rate, long-lived lava flows. Valley networks were also probably developed by the action of low-viscosity lavas, possibly by an unusual lava sapping process.

Canali-type channels are unique because of their great lengths (up to 6800 km) and nearly constant width along their paths. These dimensions require unusual eruptive conditions, most probably including an extended eruption of a large volume of channel-forming lava. If canali formed mainly by constructional processes, laminar tholeiitic flows of relatively high, sustained discharge rates might travel the observed distances, but the absence of levees or lateral flow deposits would need to be explained. An exotic low-temperature,

low-viscosity lava, such as carbonate or sulfur, seems to be required for the erosional genesis of canals.

Undulatory topography imposed on canals and sinuous rille profiles seem to be the result of tectonic activity imposed since channel formation. This implies that some of the youngest plains materials, which may have been emplaced coincident with the channels, experienced significant postemplacement tectonic deformation.

**Acknowledgments.** We benefitted from discussions with J. Kargel, J. Johnson, and R. Strom. J. Aubele and T. K. P. Gregg provided unusually thorough and helpful reviews of the initial version of this chapter. J. Langdon assisted with the preparation of Figs. 20-22. Our research was supported by a NASA Planetary Geology and Geophysics grant.

#### Editor's Note

Baker et al. have provided a Venus flyover animation on the accompanying CD-ROM. Please see CDP6C2M1.

#### REFERENCES

- Baker, V. R. 1982. *The Channels of Mars* (Austin: Univ. of Texas Press).
- Baker, V. R., and Costa, J. E. 1987. Flood power. In *Catastrophic Flooding*, eds. L. Mayer and D. Nash (Boston: Allen and Unwin), pp. 1-21.
- Baker, V. R., Kocheil, R. C., Laitly, J. E., and Howard, A. D. 1990. Spring sapping and valley development. In *Groundwater Geomorphology*, eds. C. G. Higgins and D. R. Coates, GSA SP-252 (Boulder: Geological Soc. of America), pp. 235-265.
- Baker, V. R., et al. 1992. Channels and valleys on Venus: Preliminary analysis of Magellan data. *J. Geophys. Res.* 97:13421-13444.
- Bindschadler, D. L., Schubert, G., and Kaula, W. M. 1992. Coldspots and hotspots: Global tectonics and mantle dynamics of Venus. *J. Geophys. Res.* 97:13495-13532.
- Brice, J. C. 1964. *Channel Patterns and Terraces of the Loup Rivers in Nebraska*, U. S. G. S. Prof. Paper 422-D, D1-D41.
- Bussey, D. B. J., and Guest, J. E. 1992. Erosion vs. construction: The origin of Venusian channels. In *International Colloquium on Venus*, LPI Contrib. No. 789, pp. 18-19 (abstract).
- Bussey, D. B. J., Sorenson, S.-A., and Guest, J. E. 1995. Factors influencing the capability of lava to erode its substrate: Application to Venus. *J. Geophys. Res.* 100:16941-16948.
- Carr, M. H. 1974. The role of lava erosion in the formation of lunar rilles and Martian channels. *Icarus* 22:32-43.
- Chang, H. H. 1988. *Fluvial Processes in River Engineering* (New York: J. Wiley & Sons).
- Greeley, R. 1971. Lunar Hadley Rille: Consideration of its origin. *Science* 172:722-725.

- Greeley, R., ed. 1974. *Geologic Guide to the Island of Hawaii* (Washington, D. C.: NASA).
- Gregg, T. K. P., and Greeley, R. 1993. Formation of canals: Considerations of lava types and their thermal behaviors. *J. Geophys. Res.* 98:10873-10882.
- Gregg, T. K. P., and Greeley, R. 1994. Reply. *J. Geophys. Res.* 99:17165-17167.
- Gulick, V. C. 1993. Magmatic Intrusions and Hydrothermal Systems: Implications for the Formation of Martian Fluvial Valleys. Ph.D. Thesis, Univ. of Arizona.
- Gulick, V. C., and Baker, V. T. 1993. Fluvial erosion on Mars: Implications for paleoclimatic change. *Lunar Planet. Sci. Conf.* XXIV:587-588 (abstract).
- Gulick, V. C., et al. 1991. Channels on Venus: A preliminary morphological assessment and classification. *Lunar Planet. Sci. Conf.* XXII:507-508 (abstract).
- Gulick, V. C., Baker, V. R., and Komatsu, G. 1992a. Channel and valley morphology on Venus: An updated classification. *Lunar Planet. Sci. Conf.* XXIII:465-466 (abstract).
- Gulick, V. C., Komatsu, G., and Baker, V. R. 1992b. Integrated valley systems on Venus: A comparative morphological study. *Lunar Planet. Sci. Conf.* XXIII:467-468 (abstract).
- Heacock, R. L., et al. 1966. *Ranger VIII and IX, Part II. Experimenters' Analyses and Interpretations*, NASA TR-32-800.
- Head, J. W., and Wilson, L. 1980. Lunar sinuous rille formation by thermal erosion: Eruption conditions, rates and durations. *Lunar Planet. Sci. Conf.* XI:427-429 (abstract).
- Head, J. W., and Wilson, L. 1986. Volcanic processes and landforms on Venus: Theory, predictions, and observations. *J. Geophys. Res.* 91:9407-9446.
- Head, J. W., et al. 1991. Venus volcanism: Initial analysis from Magellan data. *Science* 252:276-299.
- Head, J. W., et al. 1992. Venus volcanism: Classification of volcanic features and structures, associations, and global distribution from Magellan data. *J. Geophys. Res.* 97:13153-13197.
- Howard, A. D., Kocheil, R. C., and Holt, H. E. 1988. *Sapping Features of the Colorado Plateau*, NASA SP-491.
- Hulme, G. 1973. Turbulent lava flow and the formation of lunar sinuous rilles. *Mod. Geology* 4:107-117.
- Hulme, G. 1974. The interpretation of lava flow morphology. *Geophys. J. Roy. Astron. Soc.* 39:361-383.
- Hulme, G. 1982. A review of lava flow processes related to the formation of lunar sinuous rilles. *Geophys. Surveys* 5:245-279.
- Hulme, G., and Fielder, G. 1977. Effusion rates and rheology of lunar lavas. *Phil. Trans. Roy. Soc. London A* 285:227-234.
- Hunt, C. B. 1969. *Geologic History of the Colorado River*, U. S. G. S. Prof. Paper 669-C, 59-130.
- Huppert, H. E., and Sparks, R. S. J. 1985. Komatiites I: Eruption and flow. *J. Petrology* 26:694-725.
- Huppert, H. E., Sparks, R. S. J., Turner, J. S., and Arndt, N. T. 1984. Emplacement and cooling of komatiite lavas. *Nature* 309:19-22.
- Kargel, J. S., Fegley, B., Jr., Treiman, A., and Kirk, R. L. 1994. Carbonate-sulfate volcanism on Venus. *Icarus* 112:219-252.
- Kiefer, W. S., Richards, M. A., Hager, B. H., and Bills, B. G. 1986. A dynamic model of Venus' gravity field. *Geophys. Res. Lett.* 13:14-17.
- Komatsu, G., and Baker, V. R. 1992a. Venusian sinuous rilles. In *International Colloquium on Venus*, LPI Contrib. No. 789, pp. 60-61.
- Komatsu, G., and Baker, V. R. 1992b. Formation of Venusian channels and valleys, and styles of volcanism. *Lunar Planet. Sci. Conf.* XXIII:715-716 (abstract).

- Komatsu, G., and Baker, V. R. 1994a. Meander properties of Venusian channels. *Geology* 22:67-70.
- Komatsu, G., and Baker, V. R. 1994b. Plains tectonism on Venus: Inference from canali longitudinal profiles. *Icarus* 110:275-286.
- Komatsu, G., Kargel, J. S., and Baker, V. R. 1992a. Canali-type channels on Venus: Some genetic constraints. *Geophys. Res. Lett.* 19:1415-1418.
- Komatsu, G., Gulick, V. C., Kargel, J. S., and Baker, V. R. 1992b. Venus lava sapping valleys. *Lunar Planet. Sci. Conf. XXIII*:719-720 (abstract).
- Komatsu, G., Baker, V. R., Gulick, V. C., and Parker, T. J. 1993. Venusian channels and valleys: Distribution and volcanological implications. *Icarus* 102:1-25.
- Komatsu, G., Gulick, V. C., and Baker, V. R. 1996. Valley networks on Venus. *J. Geomorph.*, submitted.
- Leopold, L. B., and Wolman, M. G. 1957. *River Channel Patterns: Braided, Meandering, and Straight*, U. S. G. S. Prof. Paper 282-B, pp. 39-85.
- Leopold, L. B., and Wolman, M. G. 1960. River meanders. *Geol. Soc. America Bull.* 71:769-794.
- Mackin, J. H. 1948. The concept of the graded river. *Geol. Soc. America Bull.* 59:463-512.
- Mars Channel Working Group. 1983. Channels and valleys on Mars. *Geol. Soc. America Bull.* 94:1035-1054.
- McGill, G. E. 1993. Wrinkle ridges, stress domains, and kinematics of Venusian plains. *Geophys. Res. Lett.* 20:2407-2410.
- Mouginis-Mark, P. J., Wilson, L., and Zuber, M. T. 1992. The physical volcanology of Mars. In *Mars*, eds. H. H. Kieffer, B. M. Jakosky, C. W. Snyder and M. S. Matthews (Tucson: Univ. of Arizona Press), pp. 424-452.
- Murase, T., and McBirney, A. R. 1970. Viscosity of lunar lavas. *Science* 167:1491-1493.
- Murase, T., and McBirney, A. R. 1973. Properties of some common igneous rocks and their melts at high temperatures. *Geol. Soc. America Bull.* 84:3563-3592.
- Oberbeck, V. R., Quaide, W. L., and Greeley, R. 1969. On the origin of lunar sinuous rilles. *Mod. Geology* 1:75-80.
- Parker, T. J., et al. 1991. An outflow channel in Lada Terra, Venus. *Lunar Planet. Sci. Conf. XXII*:1035-1036 (abstract).
- Parker, T. J., Komatsu, G., and Baker, V. R. 1995. Kallistos Vallis, Venus: Geology of a catastrophic flood channel. In preparation.
- Phillips, R. J., Grimm, R. E., and Malin, M. C. 1991. Hot-spot evolution and the global tectonics of Venus. *Science* 252:651-658.
- Powell, J. W. 1875. *Exploration of the Colorado River of the West and Its Tributaries* (Washington, D. C.: U. S. Government Printing Office).
- Robertis, M., Guest, J. E., Guest, J. W., and Lancaster, M. G. 1992. Mylitta Fluctus, Venus: Rift-related, centralized volcanism and the emplacement of large-volume flow units. *J. Geophys. Res.* 97:15991-16015.
- Ryerson, F. J., Weed, H. C., and Piwinski, A. J. 1988. Rheology of subliquidus magmas. I. Pictic compositions. *J. Geophys. Res.* 93:3421-3436.
- Schaber, G. G., 1992. Geology and distribution of impact craters on Venus: What are they telling us? *J. Geophys. Res.* 97:13257-13302.
- Schumm, S. A., and Khan, H. R. 1972. Experimental study of channel patterns. *Geol. Soc. America Bull.* 88:1755-1770.
- Schumm, S. A., Khan, H. R., Winkley, B. R., and Robbins, L. G. 1972. Variability of river patterns. *Nature* 237:75-76.
- Senske, D. A., Saunders, R. S., Stofan, E. R., and Members of the Magellan Science Team. 1994. The global geology of Venus: Classification of landforms and geologic history. *Lunar Planet. Sci. Conf. XXV*:1245-1246 (abstract).

- Solomon, S. C., et al. 1992. Venus tectonics: An overview of Magellan observations. *J. Geophys. Res.* 97:13119-13255.
- Strom, R. G. 1965. *Interpretations of Ranger VII Records*, JPL Tech. Rept. 32, chp. III.
- Strom, R. G., Schaber, G. G., and Dawson, D. D. 1994. The global resurfacing of Venus. *J. Geophys. Res.* 99:10899-10926.
- Swanson, D. A., Wright, T. L., and Helz, R. T. 1975. Linear vent systems and estimated rates of magma production and eruption for the Yakima Basalt on the Columbia Plateau. *Amer. J. Sci.* 275:877-905.
- Treiman, A. H. 1994. Comment on "Formation of Venusian canali: Considerations of lava types and their thermal behaviors" by T. K. P. Gregg and R. Greeley. *J. Geophys. Res.* 99:17163-17164.
- Zuber, M. T. 1990. Ridge belts: Evidence for regional- and local-scale deformation on the surface of Venus. *Geophys. Res. Lett.* 17:1369-1372.
- Zuber, M. T., and Parmentier, E. M. 1990. On the relationship between isostatic elevation and the wavelengths of tectonic surface features on Venus. *Icarus* 85:290-308.

